



Neutron Measurements for Biomedical and Fusion Technology Applications

H.H. Barschall

August 1984

UWFDM-591

Prepared for Conference on Neutron Nucleus Collisions – A Probe of Nuclear Structure,
Burr Oak State Park, Glouster, OH, 5-8 September 1984 (AIP Conf. Proc. 124 (1985)
286).

FUSION TECHNOLOGY INSTITUTE

UNIVERSITY OF WISCONSIN

MADISON WISCONSIN

Neutron Measurements for Biomedical and Fusion Technology Applications

H.H. Barschall

Fusion Technology Institute
University of Wisconsin
1500 Engineering Drive
Madison, WI 53706

<http://fti.neep.wisc.edu>

August 1984

UWFDM-591

Prepared for Conference on Neutron Nucleus Collisions – A Probe of Nuclear Structure, Burr Oak State Park, Glouster, OH, 5-8 September 1984 (AIP Conf. Proc. 124 (1985) 286).

NEUTRON MEASUREMENTS FOR BIOMEDICAL AND FUSION TECHNOLOGY APPLICATIONS

H.H. Barschall

Fusion Engineering Program
Nuclear Engineering Department
University of Wisconsin-Madison
Madison, Wisconsin 53706

August 1984

UWFD-591

NEUTRON MEASUREMENTS FOR BIOMEDICAL AND FUSION TECHNOLOGY APPLICATIONS

H.H. Barschall
University of Wisconsin, Madison, Wisconsin 53706

ABSTRACT

Measurements of reaction cross sections of neutrons of energy above 5 MeV yield important information about reaction mechanisms. The main impetus for such measurements has, however, recently come from applications. Measurements on light elements are needed for neutron dosimetry, primarily for radiotherapy. Measurements on heavier nuclides provide information for fusion technology, both for the assessment of radiation damage and for the management of radioactive wastes.

INTRODUCTION

Measurements of nuclear cross sections for neutrons from thermal energy to a few MeV have yielded much information about the nucleon-nucleus interactions; they led for example to the development of the compound nucleus model and of the optical model, and provided information about the statistical properties of nuclear energy levels near 8-MeV excitation energy. In recent years there has been an interest in extending accurate cross-section measurements to higher neutron energies. These measurements also yield new information about nuclear reaction mechanisms.

One of the early important measurements at higher neutron energies was Louis Rosen's study¹ of the secondary neutron spectra from the interaction of 14-MeV neutrons with heavy nuclei. Fig. 1 shows the angular distribution of the secondary neutrons produced in the interaction of 14-MeV neutrons with Ta. The angular distribution of the neutrons of energy below 4 MeV is isotropic, while the higher energy neutrons are forward peaked. Although the results were originally not interpreted in that way, they gave the first evidence for preequilibrium processes.

Neutron cross-section measurements at energies above about 10 MeV are much more difficult than measurements at lower energy, partly because of the lack of intense sources of monoenergetic neutrons of variable higher energy, and partly because of the many reaction channels that are important. Much of the impetus for recent work in the energy region from 10 to 30 MeV has come from the needs in applications. I want to discuss two areas in which such cross section are of importance, some of the information that is needed, and some of the results that have been obtained. The two areas are radiotherapy and fusion technology.

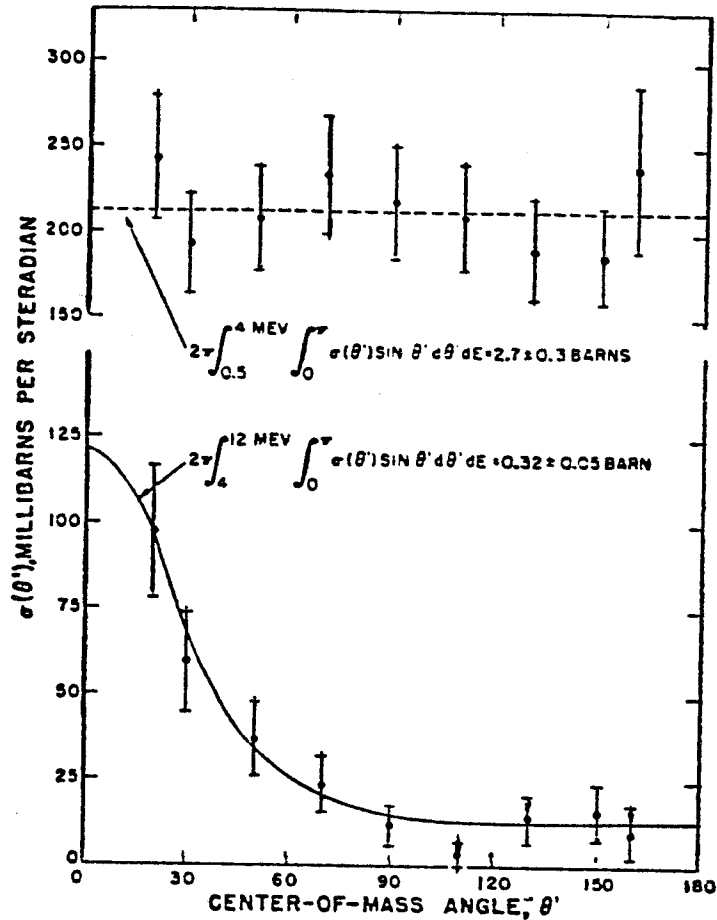


Fig. 1 Angular distribution of secondary neutrons from the interaction of 14-MeV neutrons with Ta measured in 1957. The forward peaking of the neutrons of energies between 4 and 12 MeV is the earliest evidence for preequilibrium processes. (From Reference 1).

RADIOTHERAPY

The use of high-energy neutrons in radiotherapy was proposed by E. O. Lawrence² in 1936. Between 1938 and 1943 200 cancer patients were treated with neutrons from the Berkeley cyclotron. Although there appeared to be some benefits from the treatment, many patients suffered severe side effects, and the physicians who had directed the neutron treatment concluded³ that these complications made neutron treatment an undesirable procedure. A more recent evaluation of the Berkeley treatments⁴ has shown, however, that, on the basis of our present knowledge of the biological effects of neutrons, the patients received too large doses of radiation. At the end of the fifties new radiobiological data became available which raised the hope that fast neutron therapy might cure some malignant diseases which do not respond to

conventional x-ray therapy. The clinical use of neutrons resumed in 1966 at the Hammersmith hospital in London. The reports from Hammersmith ⁵ were so encouraging that many radiotherapists began to use neutrons. There are now about two dozen neutron radiotherapy facilities in Europe, Japan, and the USA, and several thousand patients have been treated. After the initial great expectations present judgment of the advantages of neutron therapy over x-ray therapy is more guarded ⁶, but some radiotherapists think that the advantages of neutrons have been underestimated, because most facilities that have been used do not produce optimal neutron fields. In particular, higher neutron energies would produce better penetration.

DOSIMETRY

A challenge to the physicist is the determination of the neutron dose used in the treatment. If the dose is 5% too low, the treatment may be ineffective, if it is 5% too high, complications are likely to occur. As an example, Fig. 2 shows the dose-effect relationship for tumor control and for skin and intestinal damage

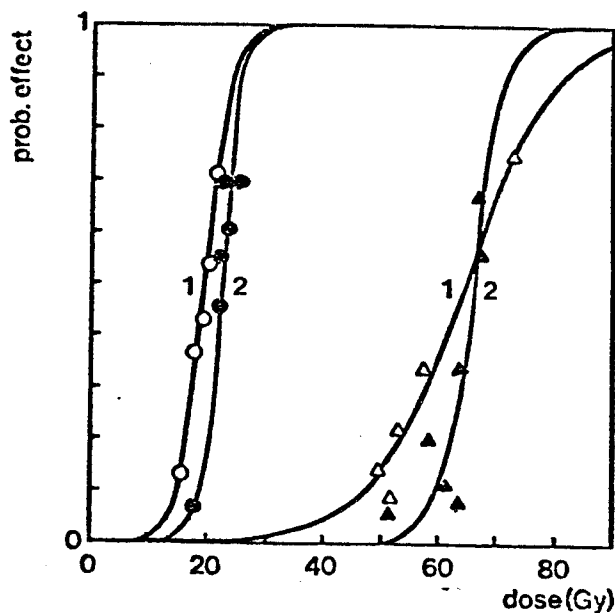


Fig. 2 Effect versus dose for tumor control (open circles) after irradiation of bladder tumors by 14-MeV neutrons. The solid circles give the corresponding results for skin and intestinal damage after neutron irradiation. Triangles show tumor control and damage, respectively, for photon irradiation. (From Reference 7).

after neutron and photon irradiation of bladder tumors ⁷. Determination of the neutron dose with an accuracy of a few percent is very difficult for several reasons: Most clinical neutron beams have continuous energy spectra extending up to 30 MeV or even 60 MeV neutron energy. In addition to neutrons, there are always γ -rays present, and the neutron dose needs to be known at the position of the tumor, i.e. inside the body where measurements can usually not be performed.

Neutron dose is defined as energy deposited per unit mass. The most direct dose measurement uses a calorimeter ⁸, but the temperature rise is so small that this method is not practical for routine clinical use. In addition, the calorimeter does not distinguish heating by neutrons and by γ -rays, but a given neutron dose has a much larger biological effect than the same γ -ray dose. Routine dose determinations are usually carried out with tissue equivalent ionization chambers ⁹, although they do not distinguish neutron and γ -ray dose either. These chambers actually measure the kinetic energy of the charged particles released by the neutrons in a plastic that has properties similar to tissue. The energy of the charged particles per unit mass is called kerma, and, for practical purposes, is the same as dose. Tissue-equivalent chambers were developed for use with x-rays. In order to make the wall of the chamber a solid conductor, plastic materials have been developed in which the oxygen in tissue, especially the oxygen in H₂O, is replaced by carbon. The problem is that for neutrons the charged-particle production per unit mass of oxygen and of carbon differ substantially, and the difference depends on neutron energy. Hence the cross sections for charged-particle production in both oxygen and carbon need to be known for the neutron spectrum used in the treatment. Unfortunately the relevant cross sections are very poorly known. As an example, Fig. 3 is taken from a recent evaluation ¹⁰ of the ¹²C cross section and shows the ¹²C(n, n₃) cross section as a function of energy. This reaction makes one of the largest contributions to the kerma and the latest two evaluations (ENDF/B-V and JENDL-3) differ by more than a factor of two at some energies between 10 and 20 MeV. Efforts to improve the data have been made at Ohio University ¹¹, UC-Davis ¹², and at Lawrence Livermore National Laboratory ¹³. As an example of the uncertainties in our knowledge of these cross sections, Table I, taken from reference 13, shows a factor of almost three between the most recent measurements of the ¹²C(n, 3 α) cross section which is the reaction that makes the largest contribution to the kerma of carbon, even though these measurements are performed at an energy of 14 MeV where measurements are easiest, since intense sources of monoenergetic neutrons are available.

Because of the unavailability of adequate cross-section data, integral kerma measurements have also been performed ¹⁴. In these measurements the energy-loss distribution of the charged particles produced by neutrons is measured in a small counter, and neutron and γ -ray induced events can be distinguished. According to a

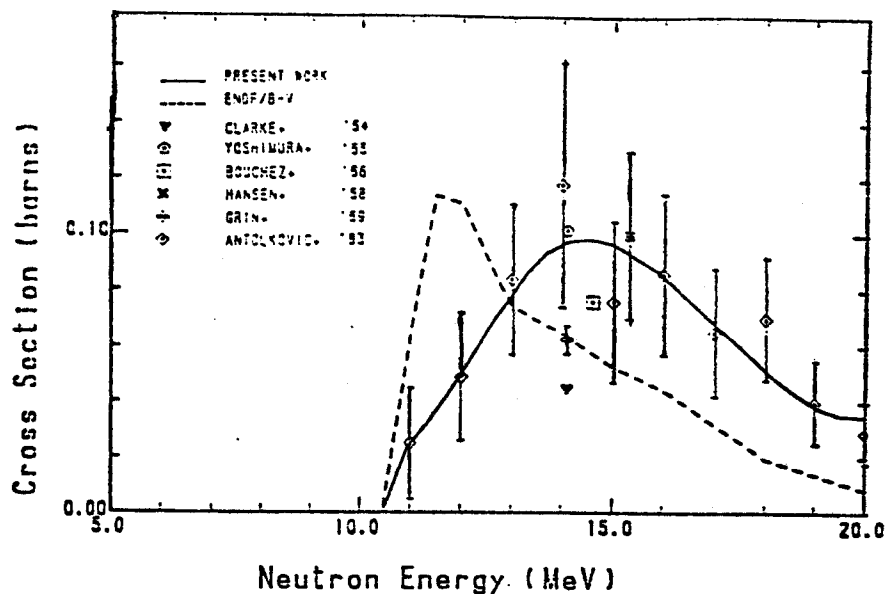


Fig. 3 Measured and evaluated cross sections for the $^{12}\text{C}(n, n_3)^3\alpha$ reaction. (From Reference 10).

theory developed by Bragg and Gray, under carefully chosen conditions the kerma in the wall of the counter can be deduced from the energy loss of charged particles in a small cavity. Suitable counters were developed by Rossi ¹⁵. The neutron flux density required for such a measurement can be readily achieved with low-current accelerators. These counters satisfy the Bragg-Gray condition more accurately for alpha particles than for carbon recoils. Preliminary results on carbon indicate that the alpha-production cross section in carbon varies rapidly with energy so that some of the discrepancies shown in Table I may be due to differences in the neutron spectra used in the measurements.

Table I
Cross Section for the Reaction $^{12}\text{C}(n, n')^3\alpha$

Year	Method	Neutron Energy (MeV)	Cross Section (mb)
1955	Emulsion	14.1	230 ± 50
1958	Emulsion	14.0	176 ± 82
1969	Scintillator	14.1	190 ± 20
1973	Scintillator	14.0	190 ± 20
1976	Scintillator	14.2	202 ± 30
1983	Emulsion	14.0	301 ± 89
1984	Quadrupole Spectrometer	14.1	110 ± 15

RADIATION DAMAGE

The other application of neutron cross-section measurements that I want to discuss is fusion technology. All near-term fusion reactor designs use the D-T reaction in which most of the energy is released in the form of 14-MeV neutrons. The first wall and other components of the reactor will be exposed to a high neutron flux density, typically $10^{14} \text{ cm}^{-2}\text{s}^{-1}$, mostly at elevated temperatures and high mechanical stresses. Under these conditions severe deterioration of many mechanical properties is expected. Although there is much information available about the radiation damage caused by fission neutrons, 14-MeV neutrons produce additional effects which cause additional damage. Most important is the very much higher rate of production of hydrogen and helium isotopes. These gases will produce swelling and embrittlement. For estimates of the useful lifetimes of various alloys a knowledge of the gas production cross section in the constituents is necessary. Although considerable progress has been made in identifying alloys that will have a relatively long useful life, such as ferritic steels ¹⁶, even the most optimistic estimates of the lifetime of the first wall of a fusion reactor is about six years. This raises the question of the disposal of the large amount of highly radioactive material that has to be replaced. Efforts have been made to estimate the amount of radioactivity that has to be disposed ^{17,18}. For this a knowledge of the reaction cross sections of all the constituents is needed for all transmutations that lead to radioactive products. This is a second reason for the interest in 14-MeV cross sections.

In some cases an activation cross section yields a gas production cross section, but not always. Because of the many reaction channels that are open, the same activity can often be produced in different reactions, and conversely starting from a given nuclide, reactions producing alpha particles, for example, can lead to different activities. Several approaches have been used to determine relevant reaction cross sections. Kneff et al. ¹⁹ have measured directly the amount of helium generated by the fast neutrons by using a mass spectrometer. This method works, however, only for helium, not for hydrogen, which is also of importance, and it does not provide information about the kerma, which is of importance both for estimating radiation damage from atomic displacements and for determining local heating by neutrons.

An extensive program of measurements of charged-particle production by 14-MeV neutrons was started at Livermore eight years ago. Similar measurements have been performed more recently at lower neutron energy at Ohio University. The problem in performing such measurements is that one needs to measure the energy distributions of all the charged particles produced, primarily protons, deuterons, and alpha particles, as a function of reaction angle, and that the measurement has to be performed in a high neutron flux where semiconductor detectors have a short life time

and a high background count rate. The procedure which was developed ²⁰ uses magnetic lenses to transport the charged particles from a radiator near the neutron source to the detectors which are several meters away and are shielded from the source. $\Delta E-E$ silicon surface barrier detectors served to identify the charged particles and to measure their energy. As an example of the energy distribution of protons, Fig. 4 shows the proton spectrum from nickel. ²¹ Just as in Rosen's early measurements of

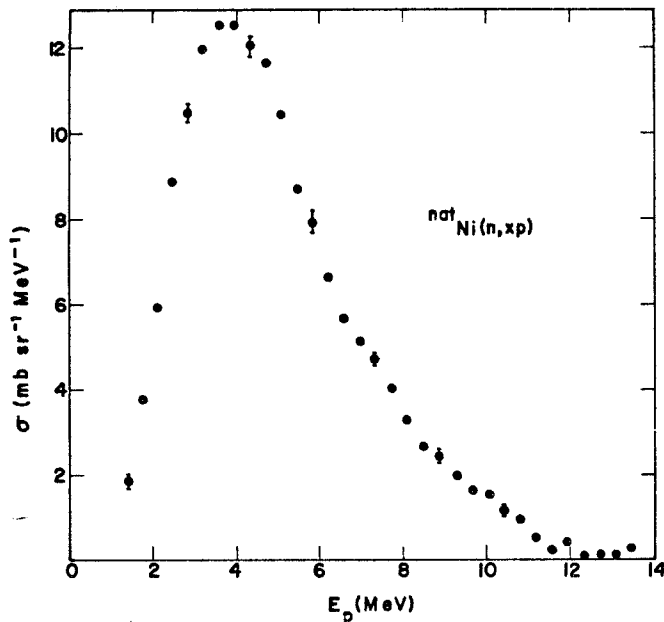


Fig. 4 Proton-emission cross section from natural nickel at 90° with respect to the incident 15-MeV neutrons. (From Reference 21).

secondary neutrons, there are many more high-energy protons than would be expected from a statistical compound nucleus model. The mechanism for their production was studied by observations at different angles. This is illustrated in Fig. 5 for charged-particle emission from ⁵⁰Cr. ²¹ The high-energy protons are peaked forward and are attributed to preequilibrium processes, while the angular distribution of the low-energy protons is isotropic. The angular distribution of energetic alpha particles is also forward peaked, and so is that of the deuterons. Fig. 6 shows proton spectra integrated over emission angle. The curves are calculations. ²⁴ The statistical calculations shown by the dashed curves reproduce all but the highest energy portion of the spectra. The dot-dashed curves account for the preequilibrium portion of the spectrum. The sum of the contributions is

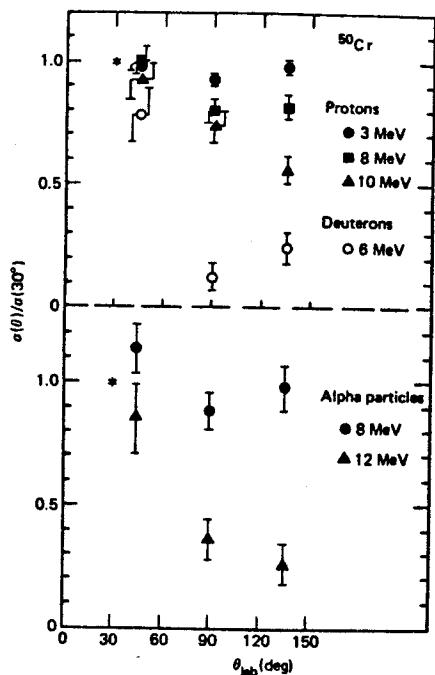


Fig. 5 Variation with angle of the cross sections for the emission of protons, deuterons, and alpha particles from the bombardment of ^{50}Cr with 15-MeV neutrons. The cross sections are normalized to unity at 30° . (From Reference 21).

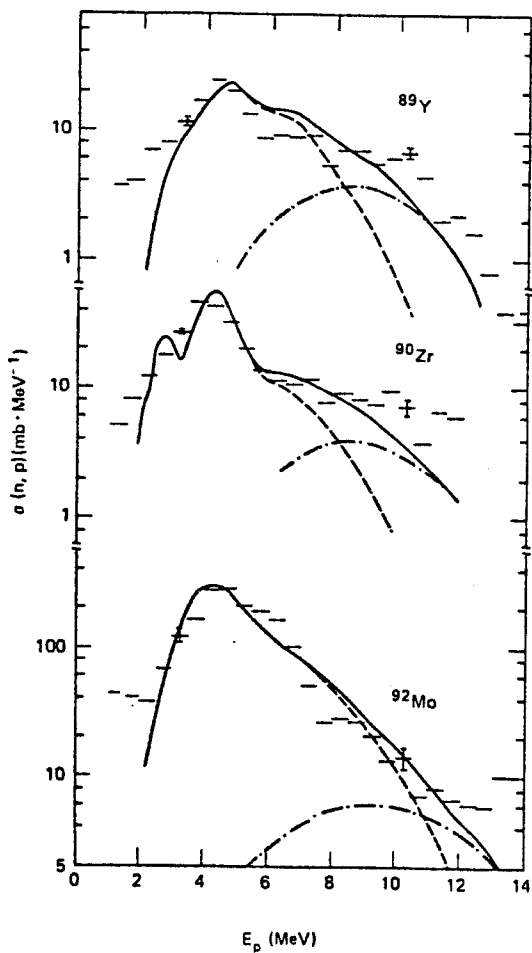


Fig. 6 Angle-integrated proton-emission cross sections for reactions induced by 15-MeV neutrons on targets of Y, ^{90}Zr , and ^{92}Mo . The dashed curves are a multistage Hauser-Feshbach calculation, the dot-dashed curves a hybrid-model calculation for preequilibrium emission, the solid curves the sum of the two. (From Reference 24).

represented by the solid curve. Addition of the preequilibrium reactions improves the fit to the data, but is not enough to account for all the observed high energy protons.

TABLE II
Cross Sections for 15-MeV Neutrons (mb)

Target	Proton Emission	Deuteron Emission	Alpha Emission	Helium Production
^{27}Al	400±60	19±8	121±25	144±7
^{46}Ti	670±90	9±4	98±18	
^{48}Ti	85±16	7±3	28±6	
^{51}V	91±14	7±3	17±3	18.7±1.4
^{50}Cr	830±100	13±4	94±15	
^{52}Cr	182±25	8±3	38±6	
^{54}Fe	900±110	10±4	80±13	91±7
^{56}Fe	190±20	8±3	41±7	46±3
^{58}Ni	1000±120	14±6	106±17	121±8
^{60}Ni	330±40	11±4	76±12	80±6
^{63}Cu	320±50	9±4	56±10	65±5
^{65}Cu	44±5	10±4	14±3	17±1
^{89}Y	98±12	10±3	8±2	
^{90}Zr	166±20	10±3	15±3	
^{93}Nb	51±8	8±3	14±3	17±5
^{92}Mo	967±116	22±7	36±7	31±2
^{94}Mo	124±15	9±3	28±6	22±2
^{95}Mo	84±10	8±3	24±5	17±1
^{96}Mo	64±8	6±2	18±4	12±1

The results of the cross section measurements for charged-particle emission induced by 15-MeV neutrons are shown in Table II for nuclides of particular interest to fusion technology. The first three columns of numbers are based on measurements with the magnetic lens spectrometer ²¹⁻²⁴, the last column is based on

helium collection. ¹⁹ For the cases where the same cross section was measured by these two very different methods the results agree quite well. Among the nuclides studied, the proton-emission cross section varies by more than an order of magnitude, while the deuteron-emission cross section is small and does not vary very much from nuclide to nuclide. The alpha-particle emission cross section, on the other hand, again varies by an order of magnitude between nuclides of interest. These measurements provide adequate information on the impact of the use of materials for fusion reactors from the point of view gas production by neutrons.

FUSION WASTE MANAGEMENT

The neutron cross sections of greatest interest to fusion technology are at present probably those for reactions that lead to long-lived radioactivities. Reference 18 lists 79 known radionuclides up to uranium with half-lives greater than five years. There may possibly be other not yet discovered long-lived radionuclides, such as products of neutron reactions with radioactive reaction products. Many of the known long-lived radionuclides can be produced in the neutron bombardment of structural materials or of impurities in these materials or of reaction products. In a fusion reactor some 500 tons of steel would be exposed to a neutron fluence of 10^{23} cm⁻² in three years of operation. Hence quite small cross sections and concentrations of impurities of a few parts per million can produce large activities. Many of the relevant cross sections are very poorly known, and present estimates of activities that have to be disposed of when the radiation-damaged structures are replaced, are based on unreliable extrapolations. I am not aware of any program of measurements of the relevant cross sections, and I think that it is an area of applied neutron physics that deserves study.

I wish to thank G.L. Kulcinski for helpful suggestions regarding the needs in fusion technology and P.M. DeLuca for discussions of neutron dosimetry.

REFERENCES

1. L. Rosen and L. Stewart, Phys. Rev. 107, 824 (1957).
2. E.O. Lawrence, Radiology 29, 313 (1937).
3. R.S. Stone, Am. J. Roentgenol. 59, 771 (1947).
4. G.E. Sheline, et al., Am. J. Roentgenol. 111, 31 (1971).
5. M. Catterall, I. Sutherland, and D.K. Bewley, Brit. Med. J. 2, 653 (1975).
6. J.J. Broerse and J.J. Battermann, Med. Phys. 8, 751 (1981).
7. J.J. Battermann, A.A. M. Hart, and K. Breur, Brit. J. Radiol. 54, 899 (1981).
8. J.C. McDonald, J.S. Laughlin, and R.E. Freeman, Med. Phys. 3, 80 (1976).

9. ICRU Report 26 "Neutron Dosimetry for Biology and Medicine," Washington (1977).
10. K. Shibata, Report NEANDC 95/U (1983).
11. A. S. Meigooni, J.S. Petler, and R.W. Finlay, Phys. Med. Biol. 29, 643 (1984).
12. T.S. Subramanian, et al., Phys. Rev. C 28, 521 (1983).
13. R.C. Haight, S.M. Grimes, R.G. Johnson, and H.H. Barschall, Nucl. Sci. Eng. 87, 41 (1984).
14. P.M. DeLuca, H.H. Barschall, R.C. Haight, and J.C. McDonald, Radiation Research (in press).
15. H.H. Rossi and W. Rosenzweig, Radiology 64, 404 (1955).
16. R.W. Powell, D.T. Peterson, M.K. Zimmerschied, and J.F. Bates, J. Nucl. Mat. 103, 104, 969 (1981).
17. F.W. Wiffen and R.T. Santaro, Proc. Conf. on Ferritic Alloys, Snowbird, Utah (1983).
18. R.C. Maninger and D.W. Dorn, Fusion Technology (to be published).
19. D.W. Kneff, B.M. Oliver, M.M. Nakata, and H. Farrar, J. Nucl. Mat. 103, 104, 1451 (1981).
20. K.R. Alvar, H.H. Barschall, R.R. Borchers, S.M. Grimes, and R.C. Haight, Nucl. Inst. Meth. 148, 303 (1978).
21. S.M. Grimes et al., Phys. Rev. C 19, 2127 (1979).
22. S.M. Grimes, R.C. Haight, and J.D. Anderson, Nucl. Sci. Eng. 62, 187 (1977).
23. S.M. Grimes, R.C. Haight, and J.D. Anderson, Phys. Rev. C 17, 508 (1978).
24. R.C. Haight, S.M. Grimes, R.G. Johnson, and H.H. Barschall, Phys. Rev. C 23, 700 (1981).